

Reentrant charge ordering transition in the manganites as experimental evidence for a strain glass

P. A. Sharma, Sung Baek Kim, T. Y. Koo,* S. Guha, and S-W. Cheong

Department of Physics & Astronomy, Rutgers University, Piscataway, New Jersey 08854, USA

(Received 21 September 2004; published 23 June 2005)

A reentrant charge ordering transition occurs within the μm -scale phase-separated manganite $(\text{La,Pr})_{5/8}\text{Ca}_{3/8}\text{MnO}_3$. This low-temperature state, in which charge-ordered and ferromagnetic-metallic phases coexist, accompanies spin-glass-like magnetism. Furthermore, thermal conductivity measurements reveal an irreversibility characteristic of a freezing transition in the *lattice* degrees of freedom, strongly suggesting the presence of inhomogeneous long-range strain. Our results point to a unique phase transition from a “strain liquid” to a “strain glass” state where phase-separated regions strongly interact via martensitic accommodation strain resulting in a cooperative freezing of the combined charge/spin/strain degrees of freedom.

DOI: 10.1103/PhysRevB.71.224416

PACS number(s): 72.80.Ga, 71.23.Cq, 75.30.Kz

Spatial phase coexistence in strongly correlated electron systems appears to be associated with a number of puzzling phenomena, including high- T_C superconductivity and colossal magnetoresistance (CMR), and surprisingly, it can happen on an astounding variety of length scales. For example, at the surface of the layered cuprates, a superconducting phase is finely mixed on the *nanoscale* with an unusual “pseudogap” phase at low temperatures (T), especially in the underdoped regime.¹ Itinerant charge carriers in the CMR manganites tend to form *nanoscale* charge-ordered (CO) regions in the insulating paramagnetic (PM) state above the ferromagnetic (FM) T .^{2,3} In addition, the spatial coexistence of metallic-FM regions with insulating-CO regions, unexpectedly, occurs on a larger, *micron-sized* length scale near the FM/CO phase boundary [in, e.g., $\text{La}_{5/8-x}\text{Pr}_x\text{Ca}_{3/8}\text{MnO}_3$ (LPCMO)].^{4,5}

This phase coexistence problem remains highly controversial, especially regarding the large length scale involved. One broad viewpoint holds that atomic-scale disorder alters the bicriticality of competing FM and CO interactions in the manganites,⁶ seemingly consistent with the fact that μm -scale phase separation (PS) occurs in systems with significant chemical substitution. However, this idea does not consider long-range strain or Coulomb interactions in a realistic way, a view difficult to reconcile with the observed μm scale. Alternatively, there is considerable evidence that martensitic accommodation strain plays a dominant role, perhaps reducing the PS problem to a manifestation of a martensitic structural transition.^{7,8}

Here we report evidence for an entirely new property of a μm -scale phase mixture in LPCMO. It appears that a system of strongly interacting (largely via strain) PS regions undergoes a cooperative, random freezing from a “dynamic” to “static” PS state reflected in the charge, spin, and lattice degrees of freedom. We label this phenomenon as a “strain glass” in analogy to a spin-glass transition.⁹ The primary distinction is that interactions between μm -scale regions are driven by long-range martensitic accommodation strain. This “strain liquid” to “strain glass” transition is signaled by a reentrance of CO as well as magnetic field (H) and T hysteresis that has clouded previous studies in this regime. Our

observations reconcile the conflicting viewpoints of PS in manganites, in that both bicriticality in the presence of atomic disorder and cooperative martensitic strain effects may be explicitly needed to explain this strain glass transition.¹⁰

Single- and polycrystalline LPCMO, with a nominal Pr content of $x \sim 0.41$, were synthesized in an optical floating zone furnace and with solid-state reaction methods, respectively. This composition is very near to the CO/FM first-order phase boundary, where μm -scale PS has been seen.⁴ The four-probe resistivity, $\rho(T)$, and thermal conductivity, $\kappa(T)$, were measured down to 2 K, and in H up to 9 T in a Quantum Design physical property measurement system. Magnetization, $M(T)$, measurements were carried out with a Quantum Design SQUID magnetometer.¹¹

In Fig. 1, we display $\rho(T)$ measured upon warming in various fixed H after zero-field cooling (ZFC) (upper panel). In zero field, $\rho(T)$ exhibits a sharp feature at ~ 210 K, indicating the PM to CO transition. Below ~ 60 K, the sample becomes too resistive to obtain accurate measurements. Even modest H produces drastic changes in this zero-field behavior. For example, for $H=8$ kOe, while CO still occurs at 210 K, $\rho(T)$ exhibits a sharp hundredfold drop at ~ 80 K. Interestingly, $\rho(T)$ suddenly increases (within <0.1 K) by several orders of magnitude at ~ 30 K, indicating a reentrance of CO. At higher H , the sharp, low T upturn tends to occur at lower T with increasing H . At still higher H (e.g., 25 kOe) this sharp upturn disappears, yet a kink in $\rho(T)$ remains.

The sharp low- T transition from the reentrant CO insulating to a more metallic state is accompanied by a large increase in M , indicating FM, shown in the lower panel of Fig. 1. At higher T , $M(T)$ sharply decreases as the CO state is recovered, with FM being lost. Finally, the CO to PM transition is also reflected by a peak in M at ~ 210 K. In the FM state, the saturation moment varies considerably for different H , nearly reaching the full, expected moment for $H=25$ kOe, as can easily be compared with the 50 kOe data. This indicates the increasing FM volume fraction as H is increased, so that FM and nonmagnetic (CO) regions coexist in this T and H regime. The $\rho(T)$ data corroborate the PS, in

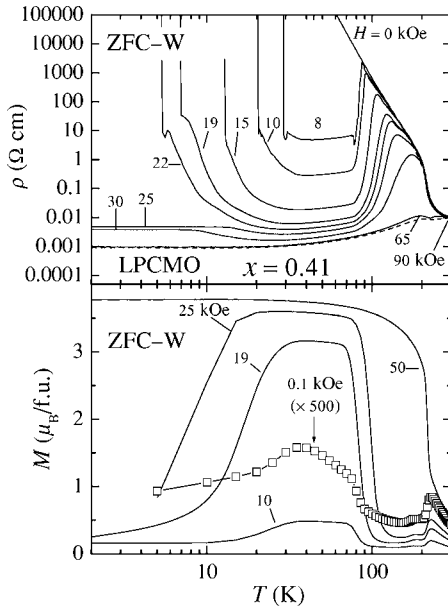


FIG. 1. Upper panel: $\rho(T)$ in various magnetic fields up to $H = 90$ kOe. For each field measurement, the sample was first cooled in zero field, then measured on warming (ZFC-W). At lower T , a reentrance of the CO state is observed. Bottom panel: ZFC-W $M(T)$ measured at various fields. Each feature in $\rho(T)$ closely corresponds with those found in $M(T)$ at each field. Open symbols denote $M(T)$ measured in very low field (0.1 kOe), magnified by 500 for clarity. Note that there is a clear sign of the CO reentrance even at this very low field.

that metallicity ($d\rho/dT > 0$) is realized at very high absolute magnitudes of ρ , a signature of percolative conduction.⁴ This same behavior is also seen *below* 30 K at high H where ρ is reduced to measurable levels, indicating electronic inhomogeneity in this regime as well. Note that the low-field (100 Oe) $M(T)$ curve continues to show sharp, well-defined anomalies consistent with the higher H data. This shows that these transitions occur even at very low, and likely in zero, H .

The above observations are succinctly summarized within the magnetic phase diagram shown in Fig. 2. Here, transitions in $\rho(T)$ and $M(T)$ from Fig. 1 were determined by peaks in $d \log(\rho)/dT$ and dM/dT , respectively, at each H . For comparison, we also show the phase boundary as determined through isothermal $M(H)$ curves (not shown), measured after ZFC to a prescribed T . The ZFC-W measurements of $\rho(T)$ and $M(T)$ roughly give consistent phase boundaries between the CO, FM, and PM phases. However, there are noticeable differences, particularly around 10–20 kOe. This may simply be due to the effects of percolative conduction in $\rho(T)$, while $M(T)$ more accurately reflects the relative volume fraction of the FM phase. Note, however, the large disagreement between the $M(H)$ phase boundary and that from $\rho(T)$ and $M(T)$. This is clearly displayed in the inset of Fig. 2, which shows the T - H phase diagram for the same sample as determined from $\rho(H)$ after ZFC (not shown), the method by which similar phase diagrams have been constructed for many other manganites.¹²

Clearly, the ZFC $\rho(H)$ or $M(H)$ considerably obscures

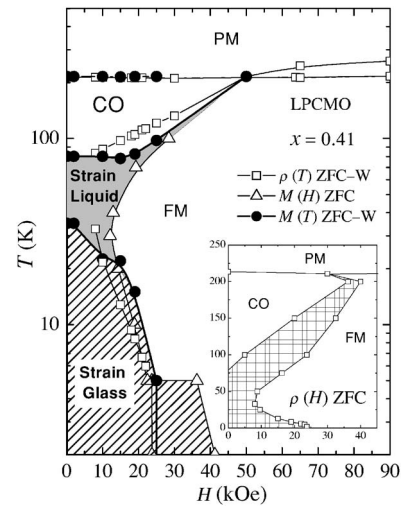


FIG. 2. The phase diagram for LPCMO, with $x=0.41$, constructed from the ZFC-W $\rho(T)$ and $M(T)$, shown in Fig. 1. Phase boundaries were ascertained from peaks in $d \log \rho(T)/dT$ (open squares), $M(H)$ curves recorded after ZFC from 300 K to the desired T (open triangles), and peaks in dM/dT (closed circle). For $T < 5$ K, sharp steps appear in the $M(H)$ curves. Note the pronounced difference between the $M(H)$ curves and the ZFC $M(T)$ data, for which the latter reveal the clear presence of a new suspected phase boundary. Inset: Corresponding phase diagram obtained solely from $\rho(H)$ curves recorded after ZFC from 300 K to the desired T . Due to the strong first-order nature of the CO to FM transition, the new phase boundary is dramatically obscured by hysteresis for ZFC $\rho(H)$ measurements.

several important aspects of this phase diagram. $M(T)$ and $\rho(T)$ measurements show the presence of an additional phase boundary at low T appearing to extend to zero H . This new boundary could signal the appearance of a new phase, which is indicated by the dashed area labeled “strain glass” (SRG). Evidently, it is difficult to detect this new phase boundary using ZFC $\rho(H)$ and $M(H)$ measurements, due to the pronounced H and T hysteresis.

In order to investigate whether $\rho(T)$ and $M(T)$ really indicate a phase transition, we have observed the effects of different field-cooling conditions: field-cooled-warming (FC-W), FC-C, as well as ZFC-W, as displayed in Fig. 3 for $H = 10$ kOe. The ZFC-W $\rho(T)$ shows a sharp decrease of ρ and increase of M at ~ 30 K. After FC, ρ is dramatically reduced at low T . However, upon warming, there is a small but noticeable further decrease of ρ at ~ 30 K, more clearly depicted in the inset of the upper panel of Fig. 3. Similarly, shown in the inset of the upper panel of Fig. 3, there is a small $\rho(T)$ drop upon FC-C at ~ 30 K. This change is less clear for FC-C, due to the large hysteresis associated with the CO to FM transition realized upon cooling ($T_C \approx 50$ K for cooling, 100 K for warming). Similar features are evident in $M(T)$ at ~ 30 K for all cases of ZFC-W, FC-C, and FC-W. The ZFC-W $\rho(T)$ behavior that suggests a reentrant CO transition below ~ 30 K could be caused by a small free-energy difference between the competing FM and CO states.¹¹ However, this comparison of the FC conditions clearly demonstrates the highly glassy nature of the charge/spin degrees of

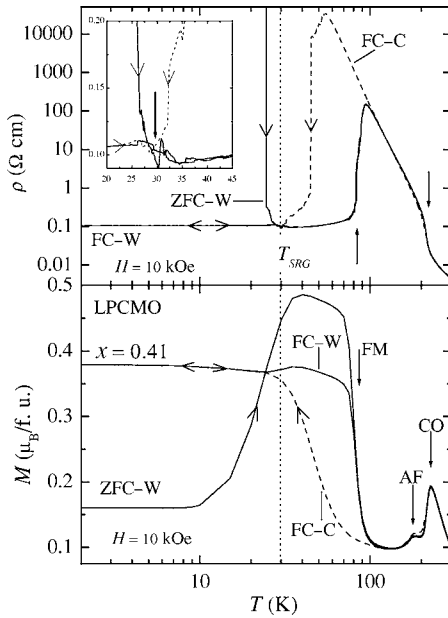


FIG. 3. $\rho(T)$ and $M(T)$ of $\text{La}_{5/8-x}\text{Pr}_x\text{Ca}_{3/8}\text{MnO}_3$, with $x=0.41$ measured under ZFC-W, FC-W, and FC-C indicated by the arrows shown. At low temperature, a new transition is proposed (~ 30 K). Note that even FC-W shows a characteristic decrease in ρ as the CO reentrance transition is traversed.

freedom, closely associated with this new inhomogeneous SRG phase.

In order to understand the lattice properties of this SRG phase, we have investigated $\kappa(T, H)$ on polycrystalline LPCMO with $x=0.4$.¹³ As can be seen in the top panel of Fig. 4, $\kappa(T)$ exhibits a number of interesting features. First, there are distinct, well-known anomalies at the FM and CO transitions, arising from (local) structural changes associated with each transition. At still lower T , there exists a slight, but noticeable, downward kink (determined by $d\kappa/dT$) at ~ 30 K where the reentrance of CO is observed in $\rho(T)$. A large positive magnetothermal conductivity is observed right after the CO to FM (high- T PS) transitions, followed by a pronounced drop at still lower T . Note that in the whole T and H range, the electronic contribution to κ , estimated from the Weidemann-Franz law, is negligible. In addition, the spin-wave κ has been shown to be insignificant in the manganites, so that the main contribution to κ should be acoustic phonons.¹⁴ We also emphasize that the system is crystalline even though the magnitude of κ at low T is comparable to that of typical glasses such as $a\text{-SiO}_2$.¹⁵

The most intriguing aspect of this result is the pronounced FC and ZFC difference in $\kappa(T)$ at various fixed H at low T , similar to that in $\rho(T)$ and $M(T)$ of Fig. 3. Very near to where the kink in $\kappa(T)$ appears, the FC and ZFC data start to differ, i.e., $\kappa(T)$ becomes *irreversible* at the SRG transition. In a spin glass, performing ZFC and then applying H at low T below the freezing temperature produces a metastable state, resulting in a lower value of χ , compared to that for FC.⁹ In this case, the ZFC metastable SRG state then has a lower value of κ as compared to FC. Evidence for such metastability, very likely strain-related, already exists. Measurements

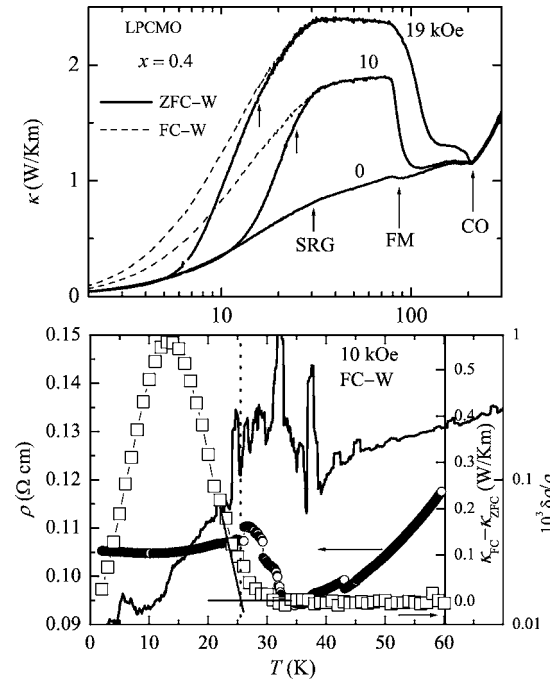


FIG. 4. Upper panel: $\kappa(T)$ measured at $H=0, 10,$ and 19 kOe for polycrystalline $\text{La}_{5/8-x}\text{Pr}_x\text{Ca}_{3/8}\text{MnO}_3$, with $x=0.4$. Solid lines indicate ZFC-W measurements. Dashed lines indicate FC-W measurements. The onset of irreversibility of the lattice $\kappa(T)$ as determined from ZFC and FC measurements indicates a spin-glass-like transition. Lower panel: ρ (open circles), $\kappa_{\text{FC}} - \kappa_{\text{ZFC}}$ (open squares), and $\delta\rho/\rho$ (lines) are shown as a function of T at 10 kOe measured upon warming. $\delta\rho/\rho$ indicates the standard deviation of the measured ρ , normalized by the magnitude of ρ . The fluctuations, quantified by $\delta\rho$, indicate the dynamic nature of the “strain liquid” phase, which then disappear at the “strain glass” transition.

of several different manganite systems at very low T show extremely sharp jumps in the $M(H)$ curves, the details of which depend on various “extrinsic” and time-dependent factors such as preparation conditions and H ramping rates.¹⁶

The lower panel of Fig. 4 illustrates these observations more clearly. Here, FC-W $\rho(T)$ is shown at 10 kOe for $x=0.41$, in comparison with the $\kappa_{\text{FC}} - \kappa_{\text{ZFC}}$ and $\delta\rho/\rho$ (the isothermal standard deviation of ρ , normalized by ρ). At the SRG transition (~ 30 K), $\rho(T)$ shows a small but sharp decrease upon warming. $\delta\rho/\rho$ is rather low below 30 K, but continually increases, showing a feature at around 30 K, and becomes large with a significant fluctuation above 30 K. Note the large T dependence of $\delta\rho/\rho$ (semilog scale) in contrast to the minimal T dependence of ρ itself, especially below 30 K. This indicates intrinsic fluctuations in ρ present above 30 K that rapidly decrease starting at 26 K. The difference between the FC and ZFC $\kappa(T)$ curves increases exactly where the noise starts to decrease.

The following observations suggest a cooperative freezing transition of phase-separated regions: (i) the sharp, well-defined features that occur in $\rho(T)$, $M(T)$, and $\kappa(T)$, consistently indicating a new phase boundary in the T - H phase diagram; (ii) spin-glass-like irreversibility between the ZFC and FC $\rho(T)$, $M(T)$, and $\kappa(T)$ at the aforementioned phase boundary; and (iii) the presence of fluctuations ($\delta\rho$) that rap-

idly disappear at the proposed “strain liquid” to “glass” transition. Note that these combined considerations suggest that the transition cannot be considered solely a reentrance of CO.¹⁷

The cross coupling of the relevant degrees of freedom is likely provided by inhomogeneous long-range strain, the presence of which is suggestive of small κ values. Fundamentally, the strain glass transition must directly couple to a stress, which is more closely analogous to H in a spin glass. In other words, H , through, e.g., magnetostriction, may act as a uniaxial stress so that ZFC and FC can now be thought of as “zero stress” cooling and “stress” cooling, respectively. In this way, the effect of a strain glass can be manifested in the properties we have measured. For example, the T hysteresis of κ could result from a greater proportion of inhomogeneous strain realized in the ZFC state, which could strongly scatter phonons due to anharmonicity.¹⁵

Strong interactions among competing PS regions, randomly nucleated by atomic-scale disorder, can occur through long-range martensitic accommodation strains, resulting from the lattice mismatch between the pseudotetragonal CO

and pseudocubic FM phases.⁷ Currently such strains are simply thought to stabilize the large-scale PS, but our results suggest that they can transform the PS state at low T , leading to a *cooperative* transition from a dynamic liquidlike to randomly frozen glasslike state. Note that our results cannot be simply explained by invoking *static* energy barriers due to strain, since this would lead to broad features in, e.g., $M(T)$, from a “slow” blocking-out process (comparable to what happens in superparamagnets¹⁸), contrary to the sharp transitions we have seen. Various irreversible sensitivity effects seem only to occur in this low- T SRG regime with μm -scale PS, such as persistent conductivity induced by photo/x-ray irradiation. Energy barriers associated with the cooperative freezing of PS regions may allow the system to “persist” in an irradiation-perturbed state in the observed highly T -dependent way.¹⁹

We thank V. Kiryukhin and A. R. Bishop for valuable discussions. This work was supported by the NSF-DMR-0405682. S.B.K. was partially supported by KOSEF.

*Present address: Pohang Accelerator Laboratory, POSTECH, Pohang, Korea.

¹S. H. Pan, J. P. O’Neal, R. L. Badzey, C. Chamon, H. Ding, J. R. Engelbrecht, Z. Wang, H. Eisaki, S. Uchida, A. K. Gupta, K.-W. Ng, E. W. Hudson, K. M. Lang, and J. C. Davis, *Nature* (London) **413**, 282 (2001).

²C. P. Adams, J. W. Lynn, Y. M. Mukovskii, A. A. Arsenov, and D. A. Shulyatev, *Phys. Rev. Lett.* **85**, 3954 (2000); P. Dai, J. A. Fernandez-Baca, N. Wakabayashi, E. W. Plummer, Y. Tomioka, and Y. Tokura, *ibid.* **85**, 2553 (2000); K. H. Kim, M. Uehara, and S-W. Cheong, *Phys. Rev. B* **62**, R11 945 (2000); B. B. Van Aken, O. D. Jurchescu, A. Meetsma, Y. Tomioka, Y. Tokura, and T. T. M. Palstra, *Phys. Rev. Lett.* **90**, 066403 (2003).

³T. Egami, *Physica C* **364-365**, 441 (2001); S. J. L. Billinge, R. G. DiFrancesco, G. H. Kwei, J. J. Neumeier, and J. D. Thompson, *Phys. Rev. Lett.* **77**, 715 (1996); A. J. Millis, Boris I. Shraiman, and R. Mueller, *ibid.* **77**, 175 (1996).

⁴M. Uehara, S. Mori, C. H. Chen, and S-W. Cheong, *Nature* (London) **399**, 560 (1999).

⁵M. Fäth, S. Freisem, A. A. Menovsky, Y. Tomioka, J. Aarts, and J. A. Mydosh, *Science* **285**, 1540 (1999).

⁶Y. Motome, N. Furukawa, and N. Nagaosa, *Phys. Rev. Lett.* **91**, 167204 (2003); D. Akahoshi, M. Uchida, Y. Tomioka, T. Arima, Y. Matsui, and Y. Tokura, *ibid.* **90**, 177203 (2003); E. Dagotto, T. Hotta, and A. Moreo, *Phys. Rep.* **344**, 1 (2001).

⁷V. Podzorov, B. G. Kim, V. Kiryukhin, M. E. Gershenson, and S-W. Cheong, *Phys. Rev. B* **64**, 140406(R) (2001).

⁸P. Littlewood, *Nature* (London) **399**, 529 (1999).

⁹J. A. Mydosh, *Spin Glasses* (Taylor and Francis, London, 1993).

¹⁰K. H. Ahn, T. Lookman, and A. R. Bishop, *Nature* (London) **428**, 401 (2004); D. I. Khomskii and K. I. Kugel, *Phys. Rev. B* **67**, 134401 (2003).

¹¹Our single-crystal sample was single-grained and showed a pseudocubic structure with a slight orthorhombic distortion. There was no obvious chemical inhomogeneity judging from our $\rho(T)$, $M(T)$, and powder x-ray-diffraction measurements. This pseudocubic system should show little anisotropy, so that all measurements were performed on a randomly cut crystal. $\rho(T)$ was measured with H perpendicular to the current direction. $\kappa(T)$ measurements were only performed on polycrystalline samples, while all other presented data correspond to measurements on single crystals.

¹²Y. Tomioka *et al.*, in *Physics of Manganites* edited by T. A. Kaplan and S. D. Mahanti (Kluwer Academic/Plenum, New York, 1999), p. 155.

¹³We have used a polycrystalline sample (showing nearly identical T - and H -dependent behavior as the first-order CO/FM boundary is crossed compared with single-crystalline LPCMO, $x \sim 0.41$) for this measurement in order to avoid problems related to cracks in large single-crystalline samples. This sample was annealed for 90 h at 1380 °C in order to achieve a large grain size, avoiding the well-known effects of such on physical properties of this system (see, e.g., Ref. 7).

¹⁴J. L. Cohn, J. J. Neumeier, C. P. Popoviciu, K. J. McClellan, and Th. Leventouri, *Phys. Rev. B* **56**, R8495 (1997); M. B. Salamon, and M. Jaime, *Rev. Mod. Phys.* **73**, 583 (2001).

¹⁵R. Berman, *Thermal Conduction in Solids* (Clarendon Press, Oxford, 1976).

¹⁶V. Hardy *et al.*, *J. Appl. Phys.* **94**, 5316 (2003); R. Mahendiran, A. Maignan, S. Hebert, C. Martin, M. Hervieu, B. Raveau, J. F. Mitchell, and P. Schiffer, *Phys. Rev. Lett.* **89**, 286602 (2002).

¹⁷S. Bogdanovich and D. Popovic, *Phys. Rev. Lett.* **88**, 236401 (2002).

¹⁸Note that the presence of static energy barriers due to strain and a “strain glass” cooperative freezing is rather akin to the difference between a superparamagnet and a canonical spin glass within our analogy.

¹⁹V. Kiryukhin, D. Kasa, J. P. Hill, B. Keimer, A. Vigliante, Y. Tomioka, and Y. Tokura, *Nature (London)* **386**, 813 (1997); T. Satoh, Y. Kikuchi, K. Miyano, E. Pollert, J. Hejtmanek, and Z. Jirak, *Phys. Rev. B* **65**, 125103 (2002).